Modelling epidemics with fractional-dose vaccination in response to limited vaccine supply

Zhimin Chen[a], Kaihui Liu[b,*], Xiuxiang Liu[a], Yijun Lou[c]

[a]*School of Mathematical Sciences, South China Normal University, Guangzhou, 510631, PR China*
[b]*Faculty of Science, Jiangsu University, Zhenjiang, Jiangsu, 212013, PR China*
[c]*Department of Applied Mathematics, The Hong Kong Polytechnic University, Hung Hom, Kowloon, Hong Kong*

Abstract

The control strategies of emergency infectious diseases are constrained by limited medical resources. The fractional dose vaccination strategy as one of feasible strategies was proposed in response to global shortages of vaccine stockpiles. Although a variety of epidemic models have been developed under the circumstances of limited resources in treatment, few models particularly investigated vaccination strategies in resource-limited settings. In this paper, we develop a two-group SIR model with incorporation of proportionate mixing patterns and n-fold fractional dose vaccination related parameters to evaluate the efficiency of fractional dose vaccination on disease control at the population level. The existence and uniqueness of the final size of the two-group SIR epidemic model, the formulation of the basic reproduction number and the relationship between them are established. Moreover, numerical simulations are performed based on this two-group vector-free model to investigate the effectiveness of n-fold fractional dose vaccination by using the emergency outbreaks of yellow fever in Angola in 2016. By employing linear and nonlinear dose-response relationships, we compare the resulting fluctuations of four characteristics of the epidemics, which are the outbreak size, the peak time of the outbreak, the basic reproduc-

[*]Kaihui Liu

Email addresses: `chenzm@m.scnu.edu.cn` (Zhimin Chen), `katrina.liu@connect.polyu.hk` (Kaihui Liu), `liuxiuxiang@m.scnu.edu.cn` (Xiuxiang Liu), `yijun.lou@polyu.edu.hk` (Yijun Lou)

tion number and the infection attack rate (IAR). For both types of dose-response relationships, dose-fractionation takes positive effects in lowering the outbreak size, delay the peak time of the outbreak, reducing the basic reproduction number and the IAR of yellow fever only when the vaccine efficacy is high enough. Moreover, five-fold fractional dose vaccination strategy may not be the optimal vaccination strategy as proposed by the World Health Organization if the dose-response relationship is nonlinear.

1. Introduction

The emergence and reemergence of various infectious diseases pose great threats to public health. The intervention and elimination of infectious diseases have aroused wide public concern. Global public health systems have implemented multiple control strategies such as providing effective treatments to infected individuals, isolating infectious individuals in lowering the transmissibility and vaccinating susceptible individuals to build herd immunity. However, these control strategies have constraints due to limited medical resources, which are embodied in the shortage of trained doctors, drugs and vaccines, insufficient hospital beds, isolation places and medical devices especially in rural areas of developing countries. The limited supply of medical resource also happens in developed countries. It was hard to access to the popular medication Tamiflu at metro pharmacies of USA during the flu epidemic in 2018 (CDC, 2018). Similar lack of drugs happened during the avian influenza epidemic in 2005 (Hayden, 2006). Consequently, the investigation on disease transmission in resource-limited settings can benefit decision-makers in optimising the utilisation of finite public health resources by assessing disease risks.

Mathematical models have played significant roles in investigating the prevention and control of infectious diseases for a long time. Researchers have

2

developed a variety of epidemic models under the circumstance of limited resources. The majority of these epidemic models are aimed at exploring the impact of limited resources in treatment by assuming an additional removal rate of each infected individual owing to the treatment, which is either continuously (Cui et al., 2008; Hu et al., 2008; Li et al., 2009; Rao et al., 2019; Rong

and Perelson, 2009; Rahman et al., 2016; Wang, 2006; Wang et al., 2012; Yan et al., 2014; Zhou and Fan, 2012; Zhang and Liu, 2008) or discontinuously (Qin et al., 2016; Wang and Ruan, 2004; Zhang et al., 2015; Zhu and Lin, 2018) dependent on the number of infective individuals and the available resources. Since the World Health Organization (WHO) regards in-patient beds density as an

important index evaluating the availability of public health services for possible infectives, several modelling studies have dedicated to the effect of the number of limited hospital beds on the control of epidemics by assuming the recovery rate as a function related to not only the number of infected individuals but also the number of hospital beds (Abdelrazec et al., 2016; Ge et al., 2015; Njankou

and Nyabadza, 2017; Shan and Zhu, 2014; Wang et al., 2018). By virtue of optimal control theory, a couple of researchers used the basic epidemic model with incorporation of either isolation, vaccination or both to explore the optimal isolation strategies of epidemics in resource-limited settings (Hansen and Day, 2011; Zhou et al., 2013).

However, few studies particularly investigated vaccination strategies in resource-limited settings even though there are plenty of epidemic models investigating the effect of vaccination strategies in controlling infectious diseases such as yellow fever (Zhao et al., 2018), influenza (Qiu and Feng, 2010; Xiao and Moghadas, 2013), pertussis (Magpantay et al., 2016), seasonal flu (Ghosh and Heffernan,

2016) and hepatitis B (Dai, 2016). Lee et al. modified a single outbreak epidemic model with nine compartments by incorporating a control function and applied the optimal control theory to identify how to optimally utilise the influenza vaccine when the vaccine supply is limited (Lee et al., 2011). A two-group *SIR* model with limited vaccination resources was studied in (Yu et al., 2018),

where the optimal vaccination control strategies for heterogeneous models were

3

explored. In order to uncover how the transmission of emerging infectious diseases is affected by limited vaccine supply, Qin et al. designed and analysed an *SIR* model with consideration of a specific nonlinear pulse vaccination strategy (Qin et al., 2013), which was completely different from above two studies. The objective of this paper is to investigate the effect of another vaccination strategy, i.e., dose-sparing vaccination strategy in case of limited vaccine stocks.

Researchers have launched long-term trials to examine the immunogenicity and safety of various types of reduced dose vaccines including poliovirus (Mohammed et al., 2010; Resik et al., 2013), influenza (Hung et al., 2012; Kúnzi et al., 2009; Wyatt et al., 2006) and yellow fever (Campi-Azevedo et al., 2014; Martins et al., 2013; Roukens et al., 2008, 2018) vaccines, which indicate that reduced dose vaccines showed equivalent immune response with that of full dose vaccines. The WHO recommend fractional dose vaccination just for emergency situations rather than routine immunisation (Vannice et al., 2018). The recent substantial outbreaks of yellow fever in Angola and the Democratic Republic of Congo in 2016 result in a global shortage of the yellow fever vaccine, which pushes the WHO to initiate five-fold fractional-dose yellow fever vaccination strategy in Kinshasa (Vannice et al., 2018). In order to advance the supporting evidence bases of fractional dose vaccination, Wu et al. provided a timely study in (Wu et al., 2016), where they used simple mathematical models describing the transmission of yellow fever to compute the infection attack rate (IAR) and check the robustness of this vaccination strategy. The mathematical model used in their work is the basic *SIR* epidemic model with homogeneous mixing, which is not appropriate for modelling the effect of vaccination as the contact and recovery patterns between vaccinated and unvaccinated individuals vary quite differently. Moreover, the basic reproduction number R_0 in their work is fixed and remains unchanged during the course of the epidemics. Hence, these limitations may affect the accuracy of their results such as the value of IAR calculated. This motivates us to propose a more reasonable modelling framework, that is, the multi-group modelling framework with consideration of heterogeneous group mixing patterns and n-fold fractional dose vaccination re-

4

lated parameters to evaluate the effectiveness of fractional dose vaccination on disease control at the population level.

The formulations of our model are derived elaborately in Section 2. Theoretical analysis involving the existence and uniqueness of the final size, the formulation of the basic reproduction number and the relationship between them are presented in Section 3. Numerical simulations are performed in Section 4 to investigate whether n-fold fractional dose yellow fever vaccination is effective in reducing the risk of yellow fever transmission in the situation of limited yellow fever vaccine stockpile. Discussions are provided in the final section.

2. Model formulation

Our model is based on the classic susceptible-infected-recovered (SIR) structure with the assumption of standard incidence type for disease transmission and ignoring the demographic processes (i.e. births and migration) (Brauer, 2008). We suppose the vaccination program is targeted at susceptible individuals only and completed before the epidemic starts. Each standard-dose vaccine is supposed to be effectively fractionized into n-fold ($1 \leq n \leq 5$). Let p be the proportion of population that standard-dose vaccines can coverage. Then, the vaccination coverage can be extended to np for n-fold fractional dosing vaccines. Let p_e denote the probability that a standard-dose vaccine takes effects (providing full or partial protection). This probability may be reduced due to fractional-dosing vaccines. We use $\varepsilon_e(n)$ to represent the ratio of the probability for a n-fold fractional dose vaccine taking effects relative to that of a standard-dose vaccine, which is dependent on n. Another pair of notations, $(p_f, \varepsilon_f(n))$, is introduced to measure the relative reduction in the probability that a successfully vaccinated individual with the fractional-dose vaccine gains full protection to that with the standard-dose vaccine.

Let $S_0 (\geq 0)$ be the number of susceptible individuals just before the vaccine program starts. In order to better describe the transmission dynamics, we classify the initial susceptible population into three classes, which are the V-

5

class of vaccinated individuals with full protection, the S_v-class of vaccinated individuals with partial protection and the S_u-class of individuals who are not vaccinated or experiencing vaccine failure (i.e., the vaccine takes no effect in protecting the vaccinated individual from infection). At time t, the number of individuals in the V-class, S_v-class and S_u-class are denoted by $V(t)$, $S_v(t)$ and $S_u(t)$ respectively. In this paper, we assume the full protection that vaccinated individuals may get does not wane during the epidemic. Consequently, there is no population flux in the V-class, which implies that the number of individuals in the V-class is fixed, i.e. $V(t) \equiv V(0) = p_e \varepsilon_e(n) p_f \varepsilon_f(n) n p S_0 = V_0 \geq 0$, for all $t \in \mathbb{R}$.
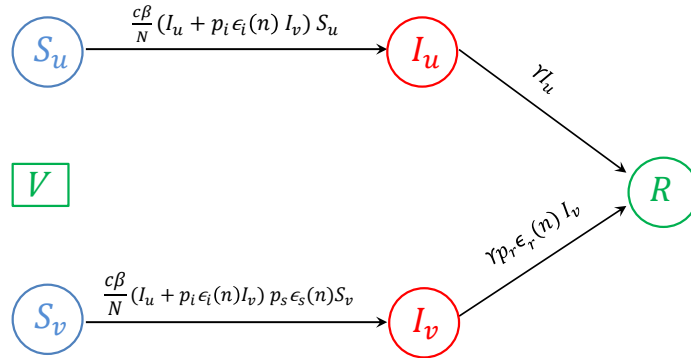

Figure 1: The transition diagram for the model with six epidemic compartments

Even though the vaccinated individuals in the S_v-class only receive partial protection, the vaccines may still play a role in reducing the susceptibility and infectiousness (Halloran et al., 1997) and increasing the recovery rate (Gandon, 2001). In order to evaluate the effects of n-fold fractional-dose vaccine, we introduce several similar pairs of notations as above, which are $(p_i, \epsilon_i(n))$, $(p_s, \epsilon_s(n))$ and $(p_r, \epsilon_r(n))$, representing the relative infectiousness, relative sus-

6

ceptibility and relative recoverability for a standard-dose and n-fold fractional-dose vaccine respectively. Detailed descriptions of the parameters are provided in Table 1. The mixing patterns between subpopulations in multi-group popu-
130 lations greatly affect the transmission of the disease (Chow et al., 2011; Yuan and Wang, 2010). In this paper, we assume the common proportionate mixing, that is, the contact probability of an individual in i-th group with the one in j-th group is in proportion to the number of contacts in j-th group (Chow et al., 2011). Thus, susceptible individuals in the S_v-class and S_u-class can get
135 infected either by the infected individuals in the I_v-class or by the infected individuals in the I_u-class. All individuals recover from infection and enter into the recovered R-class. The transfer diagram between different classes is shown in Fig. 1. The disease transition dynamics is described by a system of ordinary differential equations (ODEs) in model (2.1):

$$
\begin{cases}
\dfrac{\mathrm{d}S_u(t)}{\mathrm{d}t} = -\dfrac{c\beta}{N}\big(I_u(t) + p_i\epsilon_i(n)I_v(t)\big)S_u(t), \\[2mm]
\dfrac{\mathrm{d}I_u(t)}{\mathrm{d}t} = \dfrac{c\beta}{N}\big(I_u(t) + p_i\epsilon_i(n)I_v(t)\big)S_u(t) - \gamma I_u(t), \\[2mm]
\dfrac{\mathrm{d}S_v(t)}{\mathrm{d}t} = -\dfrac{c\beta}{N}\big(I_u(t) + p_i\epsilon_i(n)I_v(t)\big)p_s\epsilon_s(n)S_v(t), \\[2mm]
\dfrac{\mathrm{d}I_v(t)}{\mathrm{d}t} = \dfrac{c\beta}{N}\big(I_u(t) + p_i\epsilon_i(n)I_v(t)\big)p_s\epsilon_s(n)S_v(t) - \gamma p_r\epsilon_r(n)I_v(t), \\[2mm]
\dfrac{\mathrm{d}R(t)}{\mathrm{d}t} = \gamma I_u(t) + \gamma p_r\epsilon_r(n)I_v(t),
\end{cases}
\tag{2.1}
$$

140 with nonnegative initial conditions

$$
\begin{aligned}
&S_u(0) = [1 - p_e\varepsilon_e(n)np]S_0 = S_{u0}, &&I_u(0) = I_{u0}, \\[1mm]
&S_v(0) = p_e\varepsilon_e(n)(1 - p_f\varepsilon_f(n))npS_0 = S_{v0}, &&I_v(0) = I_{v0}, \\[1mm]
&R(0) = 0, &&np \leq 1.
\end{aligned}
\tag{2.2}
$$

Remark 2.1. *It is worth noting that system (2.1) can be used to investigate the impact of fractionated vaccination on vector-borne diseases. Indeed, this*

7

two-group vector-free SIR model can be reasonably deduced from a vector-host model via a quasi-equilibrium approximation approach given that the life cycle of most vectors (e.g. mosquitoes) is more rapid compared to the timescales of the epidemic and the host (Keeling and Rohani, 2008). Furthermore, it is shown that this type of vector-free SIR model may be better in parameter fitting and estimation than the vector-host model (Pandey et al., 2013).

By employing the standard ODE theory (Hale, 1980), it is not difficult to show that system (2.1) with the initial condition (2.2) is mathematically well-posed and biologically reasonable, which is summarised in the following theorem.

Theorem 2.2. *Given the initial condition* (2.2), *system* (2.1) *admits a unique nonnegative and bounded solution on* $[0, \infty)$.

Before presenting the main results of this paper, it is necessary to introduce the following notations that will be used. In order to differ the column vectors and scalars, we use bold characters to denote column vectors. Denote $\mathbb{R}^m_+ :=$ $\{\boldsymbol{X} \in \mathbb{R}^m : X_i \geq 0, i = 1, \cdots, m\}$ as the positive orthant in $\mathbb{R}^m$ and $\text{int}(\mathbb{R}^m_+) :=$ $\{\boldsymbol{X} \in \mathbb{R}^m : X_i > 0, i = 1, \cdots, m\}$ as the interior of $\mathbb{R}^m_+$. For $\boldsymbol{X}, \boldsymbol{Y} \in \mathbb{R}^m_+$, we define $\boldsymbol{X} \leq \boldsymbol{Y}$ and $\boldsymbol{Y} \geq \boldsymbol{X}$ if $\boldsymbol{Y} - \boldsymbol{X} \in \mathbb{R}^m_+$, $\boldsymbol{X} < \boldsymbol{Y}$ and $\boldsymbol{Y} > \boldsymbol{X}$ whenever $\boldsymbol{Y} - \boldsymbol{X} \in \mathbb{R}^m_+$ and $\boldsymbol{X} \neq \boldsymbol{Y}$, $\boldsymbol{X} \ll \boldsymbol{Y}$ and $\boldsymbol{Y} \gg \boldsymbol{X}$ if $\boldsymbol{Y} - \boldsymbol{X} \in \text{int}(\mathbb{R}^m_+)$. Let

$$\Lambda = \{(S_u(t), S_v(t), I_u(t), I_v(t), R(t)) \in \mathbb{R}^5_+ :$$
$$S_u(t) + I_u(t) + S_v(t) + I_v(t) + R(t) = N - V_0\},$$

where the constant N represents the number of total population, V_0 is the number of individuals in V-class, which is defined in the previous arguments. It follows from Theorem 2.2 that Λ is positively invariant for system (2.1) with initial condition (2.2).

3. Theoretical results

In this section, two important indices in controlling the spread of epidemics are investigated. One is the final size of the epidemic, which accounts for the

8

Table 1: Description of parameters in the model

Parameter	Definition	Range
c	Number of contacts per unit time an individual makes	$(0, \infty)$
β	Probability of infection given contact between a susceptible and an infected individual	$(0, 1]$
γ	Number of individuals recovered from infection per unit time without vaccine protection	$(0, \infty)$
p_e	Probability that a standard-dose vaccine takes effects	$(0, 1]$
$\epsilon_e(n)$	The ratio of the probability that a n-fold fractional-dose vaccine taking effects relative to that a standard-dose vaccine taking effects	$(0, 1]$
p_f	Probability that a successfully vaccinated individual with a standard-dose vaccine gains full protection	$(0, 1]$
$\epsilon_f(n)$	The ratio of the probability that a successfully vaccinated individual gains full protection with a n-fold fractional-dose vaccine relative to that with a standard-dose vaccine	$(0, 1]$
p_i	The ratio of the transmissibility of a vaccinated individual relative to that of an unvaccinated individual with a standard-dose vaccine	$(0, 1]$
$\epsilon_i(n)$	The ratio of the transmissibility of a vaccinated individual with an n-fold fractional-dose vaccine relative to that with a standard-dose vaccine	$[1, \infty)$
p_s	The ratio of susceptibility of a vaccinated individual relative to that of an unvaccinated individual with a standard-dose vaccine	$(0, 1]$
$\epsilon_s(n)$	The ratio of the susceptibility of a vaccinated individual with an n-fold fractional-dose vaccine relative to that with a standard-dose vaccine	$[1, \infty)$
p_r	The ratio of the recoverability of a vaccinated individual relative to that of an unvaccinated individual with a standard-dose vaccine	$[1, \infty)$
$\epsilon_r(n)$	The ratio of the recoverability of a vaccinated individual with an n-fold fractional-dose vaccine relative to that with a standard-dose vaccine	$(0, 1]$

number of individuals who actually become infected during the epidemic and who finally survive from the epidemic. This index is often considered as a critical issue in evaluating the magnitude of the epidemic. The other is the basic reproduction number, which always serves as a threshold parameter in determining whether the epidemic will break out or die out. Moreover, we establish the relationship between the final size and the basic reproduction number.

3.1. The final size

The formal statements involving expected final size of the *SIR*-epidemic model was first proposed by Kermack and McKendrick (Kermack and McKendrick, 1927). Since then, there are growing interests among researchers to formulate the final size relation for various types of epidemic models (see e.g. (Andreasen, 2011; Brauer, 2008; Ma and Earn, 2006; Magal et al., 2016, 2018; Rass and Radclie, 2003) and references therein). Among these research, both Cui et al. (Cui et al., 2018) and Magal et al. (Magal et al., 2016) proposed a similar tractable approach of establishing the final size relation for two-group *SIR* model, which motivates us to drive the final size relation of epidemic model (2.1) under the effect of n-fold fractional dosing vaccine.

In view of system (2.1), it easily follows that $S_u(t)$ and $S_v(t)$ decrease and $R(t)$ increases with respect to time $t \in \mathbb{R}$. Besides, the non-negativity and boundedness of $S_u(t)$, $S_v(t)$ and $R(t)$ imply the existence of $S_u(\infty) := \lim_{t \to \infty} S_u(t)$, $S_v(\infty) := \lim_{t \to \infty} S_v(t)$ and $R(\infty) := \lim_{t \to \infty} R(t)$. By adding the first four differential equations in system (2.1), we have

$$\frac{d}{dt}\big(S_u(t) + S_v(t) + I_u(t) + I_v(t)\big) = -\big(\gamma I_u(t) + \gamma p_r \epsilon_r(n) I_v(t)\big). \qquad (3.1)$$

Equation (3.1) implies that $S_u(t) + S_v(t) + I_u(t) + I_v(t)$ is decreasing in virtue of the nonnegativity of $I_u(t)$ and $I_v(t)$. Due to the boundedness of $I_u(t)$ and $I_v(t)$, it follows from equation (3.1) that the derivative of $S_u(t) + S_v(t) + I_u(t) + I_v(t)$ is also bounded. By letting $t \to \infty$ on both sides of equation (3.1), we have $\lim_{t \to \infty} \frac{d}{dt}\big(S_u(t) + S_v(t) + I_u(t) + I_v(t)\big) = 0$, which further indicates that $I_u(\infty) =$

10

$I_v(\infty) = 0$ on account of the nonnegativity of $I_u(t)$ and $I_v(t)$. Consequently, we have $R(\infty) = N - V_0 - S_u(\infty) - S_v(\infty)$ if the final size of the epidemic $S_u(\infty)$ and $S_v(\infty)$ are well determined.

Thus, it is imperative to establish the final size relation of the epidemics involving $S_u(\infty)$ and $S_v(\infty)$, which is summarised in the following lemma.

Lemma 3.1. *Suppose system* (2.1) *has initial conditions satisfying* $S_{u0} \gg 0$, $S_{v0} \gg 0$, *then the final sizes of susceptible populations, i.e.,* $S_u(\infty)$ *and* $S_v(\infty)$ *are determined by the following equations:*

$$
\begin{cases}
S_u(\infty) = S_{u0} \cdot \exp\Big(\dfrac{c\beta}{N\gamma} \cdot \big(S_u(\infty) - S_{u0} - I_{u0}\big) \\
\qquad\qquad + \dfrac{c\beta p_i \epsilon_i(n)}{N\gamma p_r \epsilon_r(n)} \cdot \big(S_v(\infty) - S_{v0} - I_{v0}\big)\Big), \\
S_v(\infty) = S_{v0} \cdot \exp\Big(\dfrac{c\beta p_s \epsilon_s(n)}{N\gamma} \cdot \big(S_u(\infty) - S_{u0} - I_{u0}\big) \\
\qquad\qquad + \dfrac{c\beta p_i \epsilon_i(n) p_s \epsilon_s(n)}{N\gamma p_r \epsilon_r(n)} \cdot \big(S_v(\infty) - S_{v0} - I_{v0}\big)\Big).
\end{cases}
\tag{3.2}
$$

Proof. Dividing the S_u-equation and S_v-equation in (2.1) by S_u and S_v respectively, and then integrating these two scalar equations from time 0 to t yield

$$
\begin{cases}
\ln S_u(t) - \ln S_{u0} = -\dfrac{c\beta}{N} \displaystyle\int_0^t I_u(s)\mathrm{d}s - \dfrac{c\beta p_i \epsilon_i(n)}{N} \int_0^t I_v(s)\mathrm{d}s, \\
\ln S_v(t) - \ln S_{v0} = -\dfrac{c\beta p_s \epsilon_s(n)}{N} \displaystyle\int_0^t I_u(s)\mathrm{d}s - \dfrac{c\beta p_i \epsilon_i(n) p_s \epsilon_s(n)}{N} \int_0^t I_v(s)\mathrm{d}s.
\end{cases}
\tag{3.3}
$$

It follows from the integration of the sum of S_u-equation and I_u-equation in (2.1) from time 0 to t that

$$
-\int_0^t I_u(s)\mathrm{d}s = \frac{S_u(t) + I_u(t) - S_{u0} - I_{u0}}{\gamma}.
\tag{3.4}
$$

By applying similar arguments, we have

$$
-\int_0^t I_v(s)\mathrm{d}s = \frac{S_v(t) + I_v(t) - S_{v0} - I_{v0}}{\gamma p_r \epsilon_r(n)}.
\tag{3.5}
$$

11

Substituting (3.4) and (3.5) into (3.3) gives

$$
\begin{cases}
\ln \dfrac{S_u(t)}{S_{u0}} = \dfrac{c\beta}{N\gamma} \cdot \big(S_u(t) + I_u(t) - S_{u0} - I_{u0}\big) \\
\qquad\qquad + \dfrac{c\beta p_i \epsilon_i(n)}{N\gamma p_r \epsilon_r(n)} \cdot \big(S_v(t) + I_v(t) - S_{v0} - I_{v0}\big), \\
\ln \dfrac{S_v(t)}{S_{v0}} = \dfrac{c\beta p_s \epsilon_s(n)}{N\gamma} \cdot \big(S_u(t) + I_u(t) - S_{u0} - I_{u0}\big) \\
\qquad\qquad + \dfrac{c\beta p_i \epsilon_i(n) p_s \epsilon_s(n)}{N\gamma p_r \epsilon_r(n)} \cdot \big(S_v(t) + I_v(t) - S_{v0} - I_{v0}\big).
\end{cases}
$$

On account of $I_u(\infty) = I_v(\infty) = 0$, we can easily obtain (3.2) by letting $t \to \infty$ on both sides of the above equations. $\qquad\square$

We define a map $L\colon \mathbb{R}^2 \to \mathbb{R}^2$ based on system (3.2), more specifically,

$$
L(\boldsymbol{X}) = L\left(\begin{bmatrix} x_1 \\ x_2 \end{bmatrix} \right) = \begin{bmatrix} L_1(x_1, x_2) \\ L_2(x_1, x_2) \end{bmatrix},
$$

where

$$
\begin{aligned}
L_1(x_1, x_2) &= S_{u0} \cdot \exp\Big(\frac{c\beta}{N\gamma}\big(x_1 - S_{u0} - I_{u0}\big) \\
&\quad + \frac{c\beta p_i \epsilon_i(n)}{N\gamma p_r \epsilon_r(n)}(x_2 - S_{v0} - I_{v0})\,Big)
\end{aligned}
$$

and

$$
\begin{aligned}
L_2(x_1, x_2) &= S_{v0} \cdot \exp\Big(\frac{c\beta p_s \epsilon_s(n)}{N\gamma}(x_1 - S_{u0} - I_{u0}) \\
&\quad + \frac{c\beta p_i \epsilon_i(n) p_s \epsilon_s(n)}{N\gamma p_r \epsilon_r(n)}(x_2 - S_{v0} - I_{v0}) \Big).
\end{aligned}
$$

Lemma 3.1 implies that the final size of the epidemic is well determined whenever $L(\boldsymbol{X})$ has a unique fixed point.

For simplicity, column vectors are used to represent the susceptible and infected population respectively, each of which contains both the unvaccinated and vaccinated individuals. Denote

$$
\boldsymbol{S(t)} = \begin{bmatrix} S_u(t) \\ S_v(t) \end{bmatrix} \quad \text{and} \quad \boldsymbol{I(t)} = \begin{bmatrix} I_u(t) \\ I_v(t) \end{bmatrix}.
$$

12

Thus, it follows that

$$\boldsymbol{S(0)} = \begin{bmatrix} S_{u0} \\ S_{v0} \end{bmatrix}, \qquad \boldsymbol{S(\infty)} = \begin{bmatrix} S_u(\infty) \\ S_v(\infty) \end{bmatrix},$$

and

$$\boldsymbol{I(0)} = \begin{bmatrix} I_{u0} \\ I_{v0} \end{bmatrix}, \qquad \boldsymbol{I(\infty)} = \begin{bmatrix} I_u(\infty) \\ I_v(\infty) \end{bmatrix}.$$

By applying similar arguments as in (Magal et al., 2016), it is easy to prove that $L(\boldsymbol{X})$ is monotonically increasing and strictly convex. Besides, $\boldsymbol{0} < L\big(\boldsymbol{S(0)}\big) < \boldsymbol{S(0)}$ holds. Consequently, we can deduce that $L(\boldsymbol{X})$ admits a unique fixed point $\boldsymbol{0} \ll \boldsymbol{S(\infty)} < \boldsymbol{S(0)}$, which constitutes the main result of this subsection as shown in the next theorem.

Theorem 3.2. *For system (2.1) with initial conditions (2.2), there exists a unique fixed point $\boldsymbol{S(\infty)}$ in $\big[\boldsymbol{0}, \boldsymbol{S(0)}\big]$ and $\boldsymbol{S(\infty)}$ can be determined differently on different initial conditions:*

(1) Assume $\boldsymbol{S(0)} \gg 0$ and $\boldsymbol{I(0)} > 0$, then $\boldsymbol{S(\infty)} = \lim\limits_{n\to\infty} L^n\big(\boldsymbol{0}\big)$.

(2) Assume $\boldsymbol{S(0)} \gg 0$ and $\boldsymbol{I(0)} \gg 0$, then $\boldsymbol{S(\infty)} = \lim\limits_{n\to\infty} L^n\big(\boldsymbol{S(0)}\big)$.

Remark 3.3. *Theorem 3.2 provides one possible way to numerically compute the final size of the epidemic and investigate the effects of n-fold fractional dosing vaccine on the final size.*

3.2. The basic reproduction number

The basic reproduction number is defined as the spectral radius of the next generation matrix, which denotes the expected number of individuals in the completely susceptible population infected by an infectious individual during the course of its entire infectious period (Diekmann et al., 1990). In order to establish the explicit formulation of the basic reproduction number, van den

13

Driessche and Watmough derived a straightforward expression of next generation matrix for compartmental disease models (van den Driessche and Watmough, 2002). By virtue of their theory, we obtain the next generation matrix, which is shown as follows:

$$\mathcal{G} = \begin{bmatrix} \dfrac{c\beta}{N\gamma}S_{u0} & \dfrac{c\beta p_i \epsilon_i(n)}{N\gamma p_r \epsilon_r(n)}S_{u0} \\ \dfrac{c\beta p_s \epsilon_s(n)}{N\gamma}S_{v0} & \dfrac{c\beta p_i \epsilon_i(n) p_s \epsilon_s(n)}{N\gamma p_r \epsilon_r(n)}S_{v0} \end{bmatrix}.$$

Therefore, the basic reproduction number of model (2.1)-(2.2) is

$$\mathcal{R}_0 = \rho(\mathcal{G}) = \frac{c\beta}{N\gamma}S_{u0} + \frac{c\beta \cdot p_i \cdot \epsilon_i(n) \cdot p_s \cdot \epsilon_s(n)}{N\gamma \cdot p_r \cdot \epsilon_r(n)}S_{v0}, \qquad (3.6)$$

where $\rho(\mathcal{G})$ represents the spectral radius of the next generation matrix $\mathcal{G}$.

Remark 3.4. *It is apparent that $\frac{1}{\gamma}$ and $\frac{c\beta}{N}$ represent respectively the expected* ₂₂₅ *infectious period and transmission probability for individuals without vaccine protection. In view of the impact of fractional-dose vaccines, $\frac{1}{\gamma p_r \epsilon_r(n)}$ and $\frac{c\beta}{N}p_i \epsilon_i(n)p_s \epsilon_s(n)$ denote respectively the expected infectious period and transmission probability for vaccinated individuals with n-fold fractional dose vaccines. Consequently, the first term, $\frac{c\beta}{N\gamma}S_{u0}$ and the second term, $\frac{c\beta \cdot p_i \cdot \epsilon_i(n) \cdot p_s \cdot \epsilon_s(n)}{N\gamma \cdot p_r \cdot \epsilon_r(n)}S_{v0}$,* ₂₃₀ *in equation (3.6) can be regarded as the number of new infections from unvaccinated and vaccinated group respectively infected by an infective individual, which indicates that the basic reproduction number $\mathcal{R}_0$ is counted as the addition of the reproduction numbers of unvaccinated and vaccinated groups.*

3.3. The final size relations with $\mathcal{R}_0$

In this subsection, we establish the relations between the final size of the epidemic and the basic reproduction number $\mathcal{R}_0$. Recall that we have obtained the final size equations in (3.2). Multiplying the first equation and second equation in (3.2) by S_{u0} and $\dfrac{p_i \epsilon_i(n)}{p_r \epsilon_r(n)}S_{v0}$ respectively, then adding these two

14

new equations together given the following final size relation with $\mathcal{R}_0$:

$$S_{u0} \cdot \ln \frac{S_u(\infty)}{S_{u0}} + \frac{p_i \epsilon_i(n)}{p_r \epsilon_r(n)} S_{v0} \cdot \ln \frac{S_v(\infty)}{S_{v0}}$$

$$= \mathcal{R}_0 \cdot \left[\left(S_u(\infty) - S_{u0} - I_{u0} \right) + \frac{p_i \epsilon_i(n)}{p_r \epsilon_r(n)} \cdot \left(S_v(\infty) - S_{v0} - I_{v0} \right) \right].$$

235 *3.4. Infection attack rate (IAR)*

Another significant characteristic evaluating the transmission of infectious diseases is the infection attack rate, which represents the fraction of individuals infected during the period of an epidemic (Wu et al., 2016). The infection attack rates for unvaccinated, vaccinated and total populations, denoted as $\mathcal{IAR}_u(n)$, $\mathcal{IAR}_v(n)$ and $\mathcal{IAR}(n)$ respectively, are shown as follows:

$$\begin{aligned}
\mathcal{IAR}_u(n) =& \frac{S_{u0} + I_{u0} - S_u(\infty)}{S_{u0} + I_{u0}} = 1 - \frac{S_u(\infty)}{S_{u0} + I_{u0}} \\
=& 1 - \frac{S_{u0}}{S_{u0} + I_{u0}} \exp\left(- \frac{c\beta}{N\gamma} \left[S_{u0} + I_{u0} \right] \mathcal{IAR}_u(n) \right. \\
& \left. - \frac{c\beta p_i \epsilon_i(n)}{N\gamma p_r \epsilon_r(n)} \left[S_{v0} + I_{v0} \right] \mathcal{IAR}_v(n) \right), \\
\mathcal{IAR}_v(n) =& \frac{S_{v0} + I_{v0} - S_v(\infty)}{S_{v0} + I_{v0}} = 1 - \frac{S_v(\infty)}{S_{v0} + I_{v0}} \\
=& 1 - \frac{S_{v0}}{S_{v0} + I_{v0}} \exp\left(- \frac{c\beta p_s \epsilon_s(n)}{N\gamma} \left[S_{u0} + I_{u0} \right] \mathcal{IAR}_u(n) \right. \\
& \left. - \frac{c\beta p_i \epsilon_i(n) p_s \epsilon_s(n)}{N\gamma p_r \epsilon_r(n)} \left[S_{v0} + I_{v0} \right] \mathcal{IAR}_v(n) \right),
\end{aligned}$$

and

$$
\begin{aligned}
\mathcal{IAR}(n) =& \frac{S_{u0} + I_{u0} + S_{v0} + I_{v0} - S_u(\infty) - S_v(\infty)}{S_{u0} + I_{u0} + S_{v0} + I_{v0}} \\
=& 1 - \frac{S_u(\infty) + S_v(\infty)}{S_{u0} + I_{u0} + S_{v0} + I_{v0}} \\
=& 1 - \frac{S_{u0}}{S_{u0} + I_{u0} + S_{v0} + I_{v0}} \exp\Big(- \frac{c\beta}{N\gamma} \big[S_{u0} + I_{u0} \big] \mathcal{IAR}_u(n) \\
& - \frac{c\beta p_i \epsilon_i(n)}{N\gamma p_r \epsilon_r(n)} \big[S_{v0} + I_{v0} \big] \mathcal{IAR}_v(n) \Big) - \frac{S_{v0}}{S_{u0} + I_{u0} + S_{v0} + I_{v0}} \\
& \exp\Big(- \frac{c\beta p_s \epsilon_s(n)}{N\gamma} \big[S_{u0} + I_{u0} \big] \mathcal{IAR}_u(n) \\
& - \frac{c\beta p_i \epsilon_i(n) p_s \epsilon_s(n)}{N\gamma p_r \epsilon_r(n)} \big[S_{v0} + I_{v0} \big] \mathcal{IAR}_v(n) \Big).
\end{aligned}
$$

Note that the formulations for the infection attack rate are slightly different from those in (Wu et al., 2016) due to the differences in model structures. In the following section, numerical simulations involving the n-fold fractional dose vaccine related characteristics are performed to investigate the impact of fractional dose vaccination strategy on the control of infectious diseases.

4. Numerical simulations

Motivated by the Kinshasa dose sparing yellow fever vaccination campaign in July-August 2016, the yellow fever epidemic in Kinshasa is chosen as the case study to investigate whether the n-fold fractionated vaccination campaign before the epidemic effectively control the outbreak. Yellow fever is a vector-borne disease and transmitted between humans through *Aedes aegypti* (*A. aegypti*) mosquitoes. In general, compartmental models involving both vectors and hosts are appropriate to describe vector-borne diseases. However, the main concern of this paper is to evaluate the impacts of vaccination before an epidemic by investigating variations on disease transmission between vaccinated and unvaccinated hosts. Moreover, only a small fraction of mosquitoes are involved over the course of yellow fever epidemics (Wu et al., 2016) and the vaccination strategy brings little effect on the activity of mosquitoes (WHO, 2014).

16

Thus, our grouped vector-free *SIR* model as a quasi-equilibrium approximation of describing vector-borne diseases makes sense by considering the population of mosquitoes as a constant parameter, which is embodied in the coefficients related to disease transmission.

A fraction 20% of total population (around 12.46 million) in Kinshasa are excluded from this mass vaccination campaign as they were vaccinated and gained immunity before this campaign (Wu et al., 2016). Moreover, another 0.2 million children aged between 9 months and 2 years are recommended to be given full-dose vaccines (Wu et al., 2016; Vannice et al., 2018). However, only 2.5 million standard-dose vaccines are expected to be distributed, which means the vaccination only cover around 25% of the Kinshasa population if standard-dose vaccine is given. Under the circumstance of vaccine shortage, WHO has administered 5-fold fractionated yellow fever vaccines to the rest of the population (around 9.768 million) (Wu et al., 2016). Even though there are valid supporting evidences of equal safety and immunogenicity as standard-does vaccines (Campi-Azevedo et al., 2014; Roukens et al., 2008), the effectiveness of fractional dose vaccines in protecting at-risk populations has been rarely evaluated. Wu et al. showed that 5-fold fractional dosing vaccination strategy implemented by WHO will substantially reduce the IAR of yellow fever provided that the vaccine efficacy of five-fold fractional vaccines is at least 20% (Wu et al., 2016). A linear dose-response relationship was assumed in (Wu et al., 2016). However, the relationship between the amount of fractional dose vaccine and vaccine efficacy may not be completely linear (Visser and Roukens, 2016). By comparing different (linear and nonlinear) dose-response relationships, we attempt to investigate whether n-fold fractional dose yellow fever vaccination is effective in reducing the risk of yellow fever transmission in the situation of limited yellow fever vaccine stockpile. Four key factors characterising the spread of infectious diseases are mainly concerned, which are the outbreak size of the epidemic, the peaking time of the outbreak, the infection attack rate (IAR) and the basic reproduction number R_0.

Most constant parameters of our model are obtained from literature review

17

of prior information involving the outbreak of yellow fever. The transmission ability of yellow fever between humans is closely related to the biting activity of mosquitos and the frequency of contact between humans and mosquitoes. As indicated in previous literatures (Andraud et al., 2012; Zhao et al., 2018), the biting rate is 0.5 per day per mosquito and the transition probability of each bite is 0.4, which implies that the transmission probability is $0.4 \times 0.5 = 0.2$ per mosquito per day. On account of the bites of *A. aegypti* and the environmental and climatic conditions in Africa, the average contact rate between humans through mosquitoes is fixed as 5 (Padmanabha et al., 2012). Since the average period of yellow fever infection lasts for $6 - 10$ days (Monath, 2008), we set the recovered rate as $1/8$ day^{-1}. Other constant parameters related to vaccine efficacy are estimated based on the assumptions due to lack of data. The detailed information of constant parameters and initial conditions are summarised in Table 2.

Table 2: Constant parameters and initial conditions

Symbol	Value	Unit	References
c	5	Dimensionless	(Padmanabha et al., 2012)
β	0.2	day^{-1}	(Andraud et al., 2012; Zhao et al., 2018)
γ	1/8	day^{-1}	(Andraud et al., 2012; Zhao et al., 2018)
p	0.2355	Dimensionless	Estimated
p_e	0.85	Dimensionless	Estimated
p_f	0.65	Dimensionless	Estimated
p_i	0.55	Dimensionless	Estimated
p_s	0.55	Dimensionless	Estimated
p_r	5	Dimensionless	Estimated
N	9768000	Dimensionless	Fixed
S_0	9767980	Dimensionless	Fixed
I_{u0}	20	Dimensionless	Fixed
I_{v0}	0	Dimensionless	Fixed

Parameters corresponding to the n-fold fractional dosing vaccine efficacy are determined by the dose-response relationship, which has not been explicitly confirmed up to now. The reasonable hypothesis is that the vaccine efficacy tends

not to increase with the reduced dose of fractional vaccine. The amount of anti-gen in one standard dose is assumed as 1, then the amount of antigen in an n-fold fractional dose is $1/n$, where $n \geq 1$. We denote VE(n) as the vaccine efficacy of n-fold fractional dose vaccine. For the fractionation n between n_1 (≥ 1) and n_2 (≥ 1), these vaccine efficacy related parameters are assumed to be controlled by the vaccine efficacy at its upper (VE(n_2)) and lower (VE(n_1)) bound in order to avert the overestimation of the vaccine efficacy for n-fold fractional dose. Then, the n-fold fractional vaccine efficacy related parameters ($\epsilon_e(n), \epsilon_f(n), \epsilon_r(n)$) increase with the amount of antigen in the vaccine, i.e. positively proportional to $1/n$. The following equation shows the detailed dose-response relationship:

$$\epsilon_j(n) = \text{VE}(n_2) + \left(\frac{\frac{1}{n} - \frac{1}{n_2}}{\frac{1}{n_1} - \frac{1}{n_2}} \right)^{\theta_1} \left(\text{VE}(n_1) - \text{VE}(n_2) \right), \tag{4.1}$$

$$\text{for} \quad n_1 \leq n \leq n_2 \quad \text{and} \quad j = e, f, r,$$

where θ_1 is a positive number. The other two parameters ($\epsilon_s(n), \epsilon_i(n)$) of n-fold fractional-dose vaccine show contrast relationships with the amount of antigen in the vaccine, i.e., negatively proportional to $1/n$. Then we assume

$$\epsilon_j(n) = \text{VE}(n_1) + \left(\frac{\frac{1}{n_1} - \frac{1}{n}}{\frac{1}{n_1} - \frac{1}{n_2}} \right)^{\theta_2} \left(\text{VE}(n_1) - \text{VE}(n_2) \right), \tag{4.2}$$

$$\text{for} \quad n_1 \leq n \leq n_2 \quad \text{and} \quad j = s, i,$$

where θ_2 is a positive number.

A recent study affirms that individuals receiving the one-fifth dose of yellow fever vaccines attain a long-term immunity lasting up to 10 years (Roukens et al., 2018). Hence, we assume the n-fold fractional dose vaccine can confer long-term protection without waning against yellow fever when the dose fractionation n is at most 5. Since the standard dose vaccine coverage p is 0.2355, the coverage of n-fold fractional dose vaccines is assumed as 100% when $np > 1$. It then follows from (4.1) and (4.2) that n-fold fractional dose vaccine efficacy related parameters are determined by VE(1) and VE(5) for $1 \leq n \leq 5$. The vaccine

efficacy for standard dose vaccine is assumed as 1, i.e., VE(1) = 1. Since the

benefit threshold of 5-fold fractional dose vaccine indicated in (Wu et al., 2016)
is at least 20%, we set the range of fluctuations of VE(5) as $[0.2, 1]$. Different
relationships between the dose of the fractionated vaccine and vaccine efficacy
related parameters (shown in Fig. 2) are chosen to examine the resulting vari-
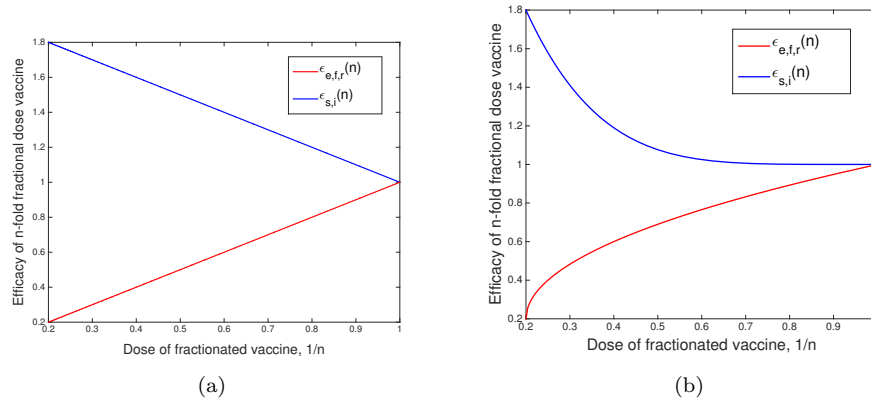ations of the effectiveness of n-fold fractional dose vaccination in the following
simulations.

(a)   (b)

Figure 2: Two different dose-response relationships for the n-fold fractional dose vaccine
efficacy related parameters. (a) Linear dose-response relationship, where $\theta_1 = \theta_2 = 1$ and the
vaccine efficacy of the maximum fold fractional vaccine is fixed VE(5) = 0.2. (b) Nonlinear
dose-response relationship, where $\theta_1 = 0.5$, $\theta_2 = 5$ and VE(5) = 0.2.

For these two different dose-response relationships, the dynamics of the total
infected population are plotted with respect to various n and VE(5) respectively.
The linear dose-response relationship is delineated in Fig. 2(a), where both θ_1
and θ_2 are set as 1 and the maximum-fold fractional-dose vaccine efficacy VE(5)
is fixed as 0.2. Under linear dose-response relationship, $n(\geq 2)$-fold fractional
dose vaccination enlarge the outbreak size for total population and bring for-
ward the peak time of the outbreak with the increase of the dose fractionation
n if the vaccine efficacy VE(5) is less than 0.6 (see Figs. 3(a)-(b)). This indi-
cates that dose-fractionation of the standard dose vaccine takes negative effects
in controlling the outbreak of yellow fever when the vaccine efficacy of n-fold
fractional dose vaccines is low. The dose-fractionation strategy plays a role in

20

delaying the outbreak and lowering down the outbreak size when the vaccine efficacy is high (see Figs. 3(c)-(d))
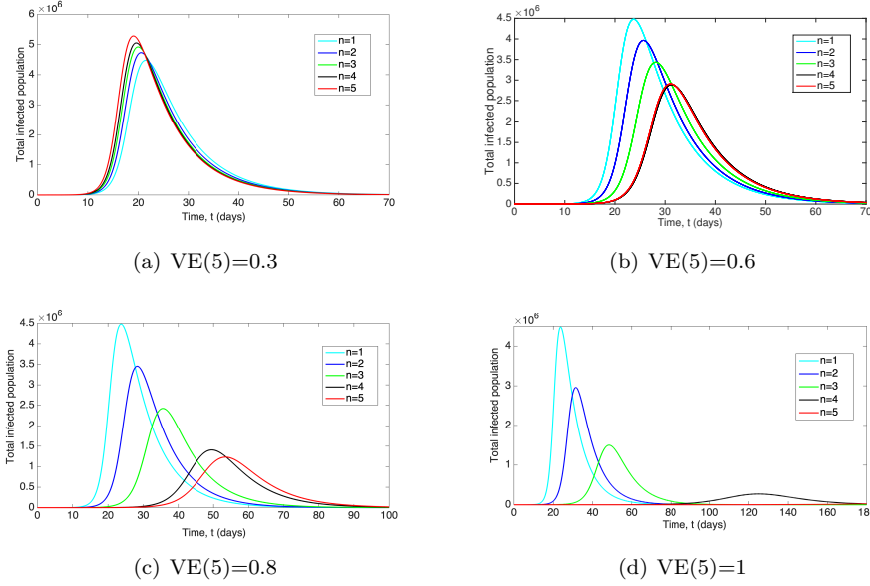

Figure 3: Dynamics for the total infected population with various dose-fractionation, n and the vaccine efficacy of maximum fold fractional vaccines, VE(5). n-fold fractional vaccine efficacy related parameters under **linear dose-response relationship**.

The situations for the case of nonlinear dose-response relationship become quite different from those under linear dose-response relationship. Fig. 2(b) shows the detailed nonlinear dose-response relationship, in which case $\theta_1 = 0.5$, $\theta_2 = 5$ and VE(5) = 0.2. Even though the vaccine efficacy VE(5) is very low, dose-fractionation is still effective in reducing the outbreak size and postponing the peak time of the outbreak as long as the fractionation n is less than 4 (see Figs. 4(a)-4(b)). However, five-fold fractional dose vaccines result in bigger outbreak size and earlier peak time with low vaccine efficacy VE(5). The effectiveness of five-fold fractional dose vaccination in lowering the risk of yellow fever becomes apparent as the vaccine efficacy VE(5) grows, while five-fold fractional dose vaccination is not the optimal strategy until the vaccine efficacy VE(5) is over 0.8 (see Figs. 4(c)-4(d)). For both dose-response relationships, the effectiveness of certain fold fractional dose vaccination in attenuating the

21

transmission of yellow fever is enhanced with increasingly higher vaccine efficacy. The outbreak of yellow fever is nearly prevented by five-fold fractional dose vaccination when the vaccine efficacy VE(5) reaches 100%.
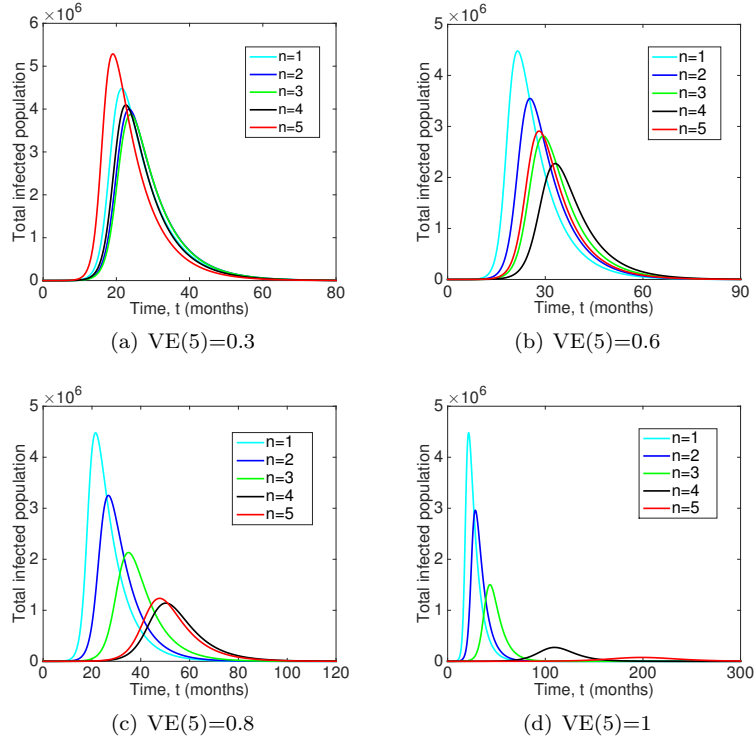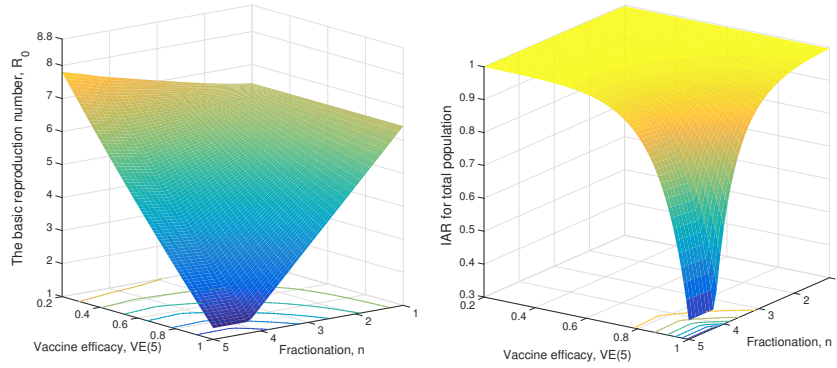

Figure 4: Dynamics for the total infected population with various dose-fractionation, n and the vaccine efficacy of maximum fold fractional vaccines, VE(5). n-fold fractional vaccine efficacy related parameters under **nonlinear dose-response relationship**.

The surfaces in Fig. 5 depict changes of R_0 and IAR with respect to the number of dose fractionation n and the maximum fold of fractionated vaccine efficacy VE(5) under two different cases of dose-response relationships. For the linear case, it is analogous to the control of the outbreak size that similar negative effects in lowering R_0 and IAR (see Fig. 5(a)) occurs if the vaccine efficacy VE(5) cannot reach 60%. In order to substantially lessen IAR, the benefit threshold of VE(5) is required to be higher than 80%. The decreasing trends in IAR and R_0 become gently whenever dose fractionation n is greater than 4

22

and the vaccine efficacy VE(5) is increasingly closer to 1. This is caused by negligible differences in the fractionated vaccine efficacy related parameters and the vaccine coverage of fractional dose vaccination. In the case of the nonlinear dose-response relationship, it can be seen from Fig. 5(b) that both R_0 and IAR decline with the increased number of dose fractionation n no matter the vaccine efficacy VE(5) is high or low. Compared with other dose fractionated vaccines, five-fold fractional dose vaccination does not optimally control the transmission until the vaccine efficacy VE(5) is higher than 0.8. Similar insignificant decline occurs as that in the linear case when $n \geq 4$ and the vaccine efficacy $VE(5)$ is raised to be close to 1.

5. Discussion

Under the circumstances of limited vaccine stockpiles, n-fold fractional dose vaccination strategy is considered as a feasible vaccination strategy in emergency epidemics. In order to model the impact of n-fold fractional vaccination strategy, we proposed a two-group SIR epidemic model with incorporating n-fold fractionated vaccines related parameters and proportionate mixing patterns. By virtue of the theories in (Magal et al., 2016; Cui et al., 2018), we established the existence and uniqueness of the final size of the epidemic for two-group SIR model, the formulation of the basic reproduction number and the relation between them. In addition to the theoretical analysis, we performed numerical simulations based on this two-group vector-free model to evaluate the effectiveness of n-fold fractional dose vaccination by using the emergency outbreaks of yellow fever in Angola. In view of our model, n-fold fractional dose vaccine related parameters are determined by the dose-response relationship. Thus, different dose-response relationships may affect the transmission dynamics. In this paper, we compared linear and nonlinear dose-response relationships and investigated the resulted fluctuations of four characteristics of the spread of infectious diseases, which are the outbreak size of the epidemic, the peaking time of the outbreak, the infection attack rate and the basic reproduction number.

23

(a) Linear dose-response relationship
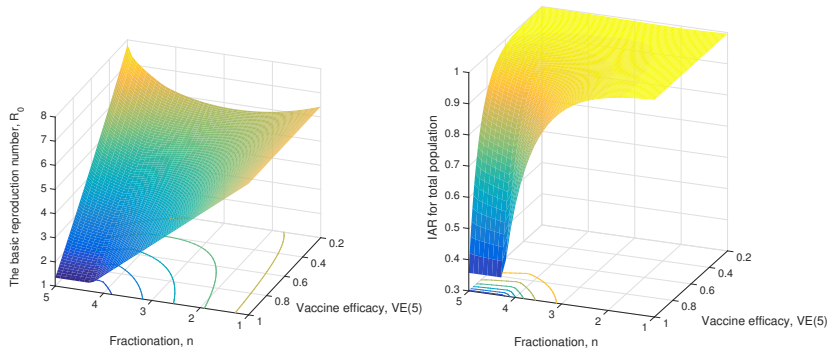
(b) Nonlinear dose-response relationship

Figure 5: The variations of the basic reproduction number R_0 and the infection attack rate (IAR) with respect to the dose-fractionation n and the vaccine efficacy VE(5). (a) n-fold fractional vaccine efficacy related parameters under linear dose-response relationship. (b) n-fold fractional vaccine efficacy related parameters under nonlinear dose-response relationship.

For both cases of dose-response relationships, we plotted the changes of these four characteristics with respect to the dose-fractionation n and the vaccine efficacy of the maximum fold dose VE(5). The numerical results indicated that dose-fractionation for both cases takes positive effects in lowering the outbreak size of yellow fever, delaying the peak time of the outbreak, reducing the IAR and R_0 when the vaccine efficacy VE(5) is high enough. The situations become different when the vaccine efficacy is low. For linear case, dose-fractionation takes negative effects in controlling the transmission of yellow fever, which is embodied in the larger IAR, R_0, outbreak size and earlier peak time of the outbreak with increased dose-fractionation when the vaccine efficacy is low. However, the effectiveness of n-fold fractional dose vaccines with nonlinear dose-response relationship is not influenced by the low vaccine efficacy. Moreover, the simulated results for nonlinear case show that five-fold fractional dose vaccination might not be the optimal vaccination strategy until the vaccine efficacy VE(5) is higher than 80%. Consequently, five-fold fractional dose vaccination implemented by WHO can prevent the transmission of yellow fever when the vaccine efficacy is high enough. Other fold of fractionation is worth considering when the vaccine efficacy is low. Public health authorities should cautiously propose the dose-sparing vaccination strategy to optimise the efficiency.

There are several limitations that may affect the accuracy of numerical results. First, our model is a two-group vector-free model, which is just an approximation to describe the transmission of vector-borne diseases by assuming the vector population as a constant parameter. However, the yellow fever is transmitted directly by mosquitoes. Thus, epidemic models incorporating dynamics of mosquitoes may be better. In the future, we will seek other infectious diseases that are directly transmitted by humans as the simulating example. Second, the parameters in the numerical simulations were fixed from literature review. Other parameterised method such as fitting from true vaccination and epidemic data may be conductive to objectively evaluate the role of vaccination strategy.

25

Acknowledgements

References

Abdelrazec, A., Belair, J., Shan, C., Zhu, H. (2016) Modeling the spread and control of dengue with limited public health resources. Math. Biosci. 136-145.

Andraud M., Hens N., Marais C. and Beutels P., 2012. Dynamic epidemiological models for dengue transmission: A systematic review of structural approaches. PLoS One 7(11):e49085.

Andreasen, V., 2011. The final size of an epidemic and its relation to the basic reproduction number. Bull. Math. Biol. 73(10):2305-2321.

Brauer, F., 2008. Epidemic models with heterogeneous mixing and treatment. Bull. Math. Biol. 70(7): 1869-1885.

Brauer, F., 2008. Compartmental models in epidemiology. In *Mathematical Epidemiology. Editors: Brauer, F., van den Driessche, P., Wu, J.*, pp. 19-79, Springer, Berlin, Heidelberg.

Campi-Azevedo, A.C., de Almeida Estevam P., Coelho-Dos-Reis J.G., et al., 2014. Subdoses of 17DD yellow fever vaccine elicit equivalent virological/immunological kinetics timeline. BMC Infect. Dis. 14:391.

Chow, L., Fan, M., Feng, Z., 2011. Dynamics of a multigroup epidemiological model with group-targeted vaccination strategies. J. Theor. Biol. 291, 56-64.

Cui, J., Mu, X., Wan, H., 2008. Saturation recovery leads to multiple endemic equilibria and backward bifurcation. J. Theor. Biol. 254(2), 275-283.

Cui, J., Zhang, Y., Feng, Z., 2018. Influence of non-homogeneous mixing on final epidemic size in a meta-population model. J. Biol. Dynam. 1-16.

Diekmann, O., Heesterbeek, J.A.P., Metz, J.A.J., 1990. On the definition and the computation of the basic reproduction ratio R_0, in models for infectious diseases in heterogeneous populations. J. Math. Biol. 28(4):365-382.

Dai, C., Fan, A., Wang, K., 2016. Transmission dynamics and the control of hepatitis B in China: A population dynamics view. J. Appl. Anal. Comput. 6(1), 76-93.

Gandon, S., Mackinnon, M.J., Nee, S., Read, A.F., 2001. Imperfect vaccines and the evolution of pathogen virulence. Nature 414(6865): 751-755.

Ghosh S., Heffernan J.M., 2016. Long-term potential of imperfect seasonal flu vaccine in the presence of natural immunity. BIOMAT 2015: International Symposium on Mathematical and Computational Biology 21-39.

Ge, J., Kim, K. I., Lin, Z., Zhu, H., 2015. A SIS reaction-diffusion-advection model in a low-risk and high-risk domain. J. Differ. Equations 259(10), 5486-5509.

Hansen, E., Day, T., 2011. Optimal control of epidemics with limited resources. J. Math. Biol., 62(3), 423-451.

Halloran, M.E., Struchiner, C.J., Longini Jr, I.M., 1997. Study designs for evaluating different efficacy and effectiveness aspects of vaccines. Am. J. Epidemiol. 146(10), 789-803.

Hale, J.K., 1980. *Ordinary differential equations*, Robert E. Krieger Publishing Company, Inc., Huntington, New York.

Hayden, F.G., 2006. Antiviral resistance in influenza viruses: Implications for management and pandemic response. New Engl. J. Med. 354(8), 785-788.

27

480   Hung, I.F., Levin, Y., To, K.K., Chan, K.H., Zhang, A.J., Li, P., et al., 2012. Dose sparing intradermal trivalent influenza (2010/2011) vaccination overcomes reduced immunogenicity of the 2009 H1N1 strain. Vaccine 30(45), 6427-6435.

Hu, Z., Liu, S., Wang, H., 2008. Backward bifurcation of an epidemic model
485   with standard incidence rate and treatment rate. Nonlinear Anal.-Real 9(5), 2302-2312.

Li, X., Li, W., Ghosh, M., 2009. Stability and bifurcation of an SIR epidemic model with nonlinear incidence and treatment. Appl. Math. Comput. 210(1), 141-150.

490   Lee, S., Morales, R., Castillo-Chavez, C., 2011. A note on the use of influenza vaccination strategies when supply is limited. Math. Biosci. Eng. 8(1), 171-182.

Kermack, W.O., McKendrick, A.G., 1927. A contribution to the mathematical theory of epidemics. Proc. R. Soc. Lond. Ser. A 115, 700-721.

495   Keeling, M. J., Rohani, P., 2008. Modeling Infectious Diseases in Humans and Animals, Princeton University Press, Princeton.

Kúnzi, V., Klap, J. M., Seiberling, M. K., Herzog, C., Hartmann, K., et al., 2009. Immunogenicity and safety of low dose virosomal adjuvanted influenza vaccine administered intradermally compared to intramuscular full dose ad-
500   ministration. Vaccine 27(27), 0-3567.

Mohammed, A.J., Alawaidy, S., Bawikar, S., Kurup, P.J., Elamir, E., Shaban, M.M.A., et al., 2010. Fractional doses of inactivated poliovirus vaccine in Oman. New Engl. J. Med. 362(25), 2351-2359.

Magal, P., Seydi, O., Webb, G., 2016. Final size of an epidemic for a two-group
505   SIR model. SIAM J. Appl. Math. 76(5), 2042-2059.

Magal, P., Seydi, O., Webb, G., 2018. Final size of a multi-group SIR epidemic model: Irreducible and non-irreducible modes of transmission. Math. Biosci. 301:59-67.

Ma, J., Earn, D.J.D., 2006. Generality of the final size formula for an epidemic of a newly invading infectious disease. Bull. Math. Biol. 679-702.

Magpantay, F.M.G., Domenech De Cellès, M., Rohani, P., King, A.A., 2016. Pertussis immunity and epidemiology: Mode and duration of vaccine-induced immunity. Parasitology 143(07), 835-849.

Martins, R.M., Maia, M.D., Farias, R.H., Camacho, L.A., Freire, M.S., Galler, R., et al., 2013. 17dd yellow fever vaccine: A double blind, randomized clinical trial of immunogenicity and safety on a dose-response study. Hum. Vaccin. Immunother. 9(4), 879-888.

Monath, T.P., 2008. Treatment of yellow fever. Antivir. Res. 78, 116–24.

Njankou, S.D., Nyabadza, F., 2017. Modelling the potential role of media campaigns in Ebola transmission dynamics. International Journal of Differential Equations. 1-13.

Padmanabha, H., Durham, D.P., Correa, F., Diukwasser, M.A., Galvani, A.P., 2012. The interactive roles of *Aedes aegypti* super-production and human density in dengue transmission. PLOS Neglect. Trop. D. 6(8), e1799.

Pandey A., Mubayi A., Medlock J., 2013. Comparing vector-host and SIR models for dengue transmission. Math. Biosci., 246(2):252-259.

Qiu, Z., Feng, Z., 2010. Transmission dynamics of an influenza model with vaccination and antiviral treatment. B. Math. Biol. 72(1), 1-33.

Qin, W., Tang, S., Cheke, R.A., 2013. Nonlinear pulse vaccination in an SIR epidemic model with resource limitation. Abstr. Appl. Anal. 2013, 670263.

Qin, W., Tang, S., Xiang, C., Yang, Y., 2016. Effects of limited medical resource on a Filippov infectious disease model induced by selection pressure. Appl. Math. Comput. 339-354.

Rass, L., Radclie, J., 2003. *Spatial deterministic epidemics*. AMS Translations of Math Monographs, 102, 261.

Rao, F., Mandal, P.S., Kang, Y., 2019. Complicated endemics of an SIRS model with a generalized incidence under preventive vaccination and treatment controls. Appl. Math. Model. 67, 38-61.

Rong, L., Perelson, A.S., 2009. Modeling HIV persistence, the latent reservoir, and viral blips. J. Theor. Biol. 260(2), 308-331.

Resik, S., Tejeda, A., Sutter, R.W., Diaz, M., Sarmiento, L., et al., 2013. Priming after a fractional dose of inactivated poliovirus vaccine. New Engl. J. Med. 368(5), 416-424.

Roukens, A.H., Vossen, A.C., Bredenbeek, P.J., van Dissel, J.T., Visser, L.G., 2008. Intradermally administered yellow fever vaccine at reduced dose induces a protective immune response: A randomized controlled non-inferiority trial. PLoS One 3:e1993.

Roukens A.H., van Halem K., de Visser A.W., Visser L.G., 2018. Long-term protection after fractional-dose yellow fever vaccination: Follow-up study of a randomized, controlled, noninferiority trial. Ann. Intern. Med. 169:761-765. doi: 10.7326/M18-1529

Rahman, A.S.M., Vaidya, N.K., Zou, X., 2016. Impact of early treatment programs on HIV epidemics: An immunity-based mathematical model. Math. Biosci., S002555641630092X.

Shan, C., Zhu, H., 2014. Bifurcations and complex dynamics of an SIR model with the impact of the number of hospital beds. J. Differ. Equations 257(5), 1662-1688.

Transcript for CDC Update on Flu Activity: https://www.cdc.gov/media/releases/2018/t0202-flu-update-activity.html.

Visser, L.G., Roukens, A.H., 2016. Modelling a way out of yellow fever. Lancet 388(10062), 2847-2848.

van den Driessche, P., Watmough, J., 2002. Reproduction numbers and sub-threshold endemic equilibria for compartmental models of disease transmission. Math. Biosci. 180, 29-48.

Vannice, K., Wilder-Smith, A., Hombach, J., 2018. Fractional-dose yellow fever vaccination-advancing the evidence base. New Engl. J. Med. 379(7), 603-605.

Wang, W., 2006. Backward bifurcation of an epidemic model with treatment. Math. Biosci. 201(1), 58-71.

Wang, W., Ruan, S., 2004. Bifurcations in an epidemic model with constant removal rate of the infectives. J. Math. Anal. Appl. 291(2), 775-793.

Wu, J.T., Peak, C.M., Leung, G.M., Lipsitch, M., 2016. Fractional dosing of yellow fever vaccine of extend supply: A modelling study. Lancet 388(10062), 2904-2911.

World Health Organization. Rapid field entomological assessment during yellow fever outbreaks in Africa. WHO: Geneva, Switzerland, 2014.

Wang, J., Liu, S., Zheng, B., Takeuchi, Y., 2012. Qualitative and bifurcation analysis using an SIR model with a saturated treatment function. Math. Comput. Model. 55(3), 710-722.

Wyatt, K.N., Ryan, G.J., Sheerin, K.A., 2006. Reduced-dose influenza vaccine. Ann. Pharmacother. 40(9), 1635-1639.

Wang, A., Xiao, Y., Zhu, H., 2018. Dynamics of a Filippov epidemic model with limited hospital beds. Math. Biosci. Eng. 15(3), 739-764.

Xiao, Y., Moghadas, S.M., 2013. Impact of viral drift on vaccination dynamics and patterns of seasonal influenza. BMC Infect. Dis. 13(1), 589.

Yu, T., Cao, D., Liu, S., 2018. Epidemic model with group mixing: stability and optimal control based on limited vaccination resources. Commun. Nonlinear Sci. 61, 54-70.

Yan, C., Jia, J., Jin, Z., 2014. Dynamics of an SIR epidemic model with information variable and limited medical resources revisited. Discrete Dyn. Nat. Soc. 1-11.

Yuan, Z., Wang, L., 2010. Global stability of epidemiological models with group mixing and nonlinear incidence rates. Nonlinear Anal.-Real 11(2), 995-1004.

Zhou, L., Fan, M., 2012. Dynamics of an SIR epidemic model with limited medical resources revisited. Nonlinear Anal.-Real 13(1), 312-324.

Zhang, X., Liu, X., 2008. Backward bifurcation of an epidemic model with saturated treatment function. J. Math. Anal. Appl. 348(1), 433-443.

Zhu, M., Lin, Z., 2018. The impact of human activity on the risk index and spatial spreading of dengue fever. Nonlinear Anal.-Real 39, 424-450.

Zhang, T., Kang, R., Wang, K., Liu, J., 2015. Global dynamics of an SEIR epidemic model with discontinuous treatment. Adv. Differ. Equ.-Ny. 2015(1).

Zhao, S., Stone, L., Gao, D., He, D., Modelling the large-scale yellow fever outbreak in Luanda, Angola, and the impact of vaccination. PLoS Neglect. Trop. D. 12(1), e0006158.

Zhou, Y., Wu, J., Wu, M., 2013. Optimal isolation strategies of emerging infectious diseases with limited resources. Math. Biosci. Eng. 10(5/6), 1691-1701.